Diagnostics for the Plasma Liner Experiment[a)]

A. G. Lynn,[1,b)] E. Merritt,[1] M. Gilmore,[1] S. C. Hsu,[2] F. D. Witherspoon,[3] and J. T. Cassibry[4]
[1]*University of New Mexico, Albuquerque, New Mexico 87131, USA*
[2]*Los Alamos National Laboratory, Los Alamos, New Mexico 87545, USA*
[3]*HyperV Technologies Corp., Chantilly, Virginia 20151, USA*
[4]*The University of Alabama, Huntsville, Alabama 35899, USA*

(Presented 19 May 2010; received 15 May 2010; accepted 18 May 2010; published online 15 October 2010)

The goal of the Plasma Liner Experiment (PLX) is to explore and demonstrate the feasibility of forming imploding spherical "plasma liners" via merging high Mach number plasma jets to reach peak liner pressures of ~0.1 Mbar using ~1.5 MJ of initial stored energy. Such a system would provide HED plasmas for a variety of fundamental HEDLP, laboratory astrophysics, and materials science studies, as well as a platform for experimental validation of rad-hydro and rad-MHD simulations. It could also prove attractive as a potential standoff driver for magnetoinertial fusion. Predicted parameters from jet formation to liner stagnation cover a large range of plasma density and temperature, varying from $n_i \sim 10^{16}$ cm^{-3}, $T_e \approx T_i \sim 1$ eV at the plasma gun mouth to $n_i > 10^{19}$ cm^{-3}, $T_e \approx T_i \sim 0.5$ keV at stagnation. This presents a challenging problem for the plasma diagnostics suite which will be discussed.
[doi:10.1063/1.3478116]

I. INTRODUCTION

Magnetoinertial fusion (MIF) (Ref. 1) utilizes a magnetized target plasma in an inertial fusion configuration in order to reduce thermal transport and increase alpha particle self-heating. This reduces the required implosion velocity to achieve ignition and a given energy gain.[2] Magnetized target fusion (MTF) is an MIF scheme that utilizes a pulsed power-driven imploding solid "liner" (Z-pinch or theta-pinch) to compress and heat an approximately few centimeter scale compact toroid (CT) target plasma, such as a field reversed configuration to thermonuclear conditions.[3] MTF may provide a relatively fast and cheap path to fusion energy gain, having vastly simplified implosion driver technology requirements as compared to inertial confinement fusion (ICF) systems, and much less complexity in general than magnetic fusion energy systems. For example, it has been estimated that repetition rates required for an MTF reactor with $Q=10$ would be ~0.1 shot/s, as compared to ~10 shots/s for ICF.[4] However, engineering a solid liner implosion system for MTF has a number of inherent technological challenges, including mechanical handing of macroscopic solid metal liners (scale: $L \sim 10$ cm and $R=5$ cm), clearing the reactor chamber to sufficient vacuum between shots, and providing sufficient "standoff" from heat and neutron fluxes for liner support and pulsed power delivery systems to survive many shots. In order to overcome the technology challenges of solid liner systems, a plasma liner system utilizing a spherical array of dense, high mass, hypervelocity plasma jets has been proposed.[5] Such a system is illustrated in Fig. 1.

As shown, a CT target plasma is formed remotely, and translated to the implosion region via pulsed coils. Plasma guns are then utilized to generate a spherical array of plasma jets, which would merge together to form a continuous, converging plasma shell (liner). This plasma liner would compress and heat the target CT plasma via PdV work and shocks. A plasma liner driven magnetoinertial fusion (PLMIF) reactor would require multimillibar converged liner stagnation pressures. In order to demonstrate the feasibility of forming a uniform converging plasma liner, the Plasma Liner Experiment (PLX) is currently beginning construction at Los Alamos National Laboratory. This is a phased project, whose ultimate goal is to demonstrate uniform, well-formed plasma liners reaching peak stagnation pressures of 0.1 Mbar. The PLX, illustrated in Fig. 2, will utilize 30 guns to form the plasma liner. The plasma guns, being developed

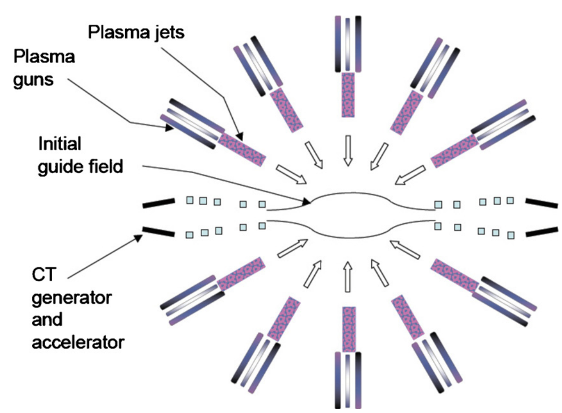

FIG. 1. (Color online) Conceptual illustration of PLMIF.

[a)]Contributed paper, published as part of the Proceedings of the 18th Topical Conference on High-Temperature Plasma Diagnostics, Wildwood, New Jersey, May 2010.
[b)]Author to whom correspondence should be addressed. Electronic mail: lynn@ece.unm.edu.

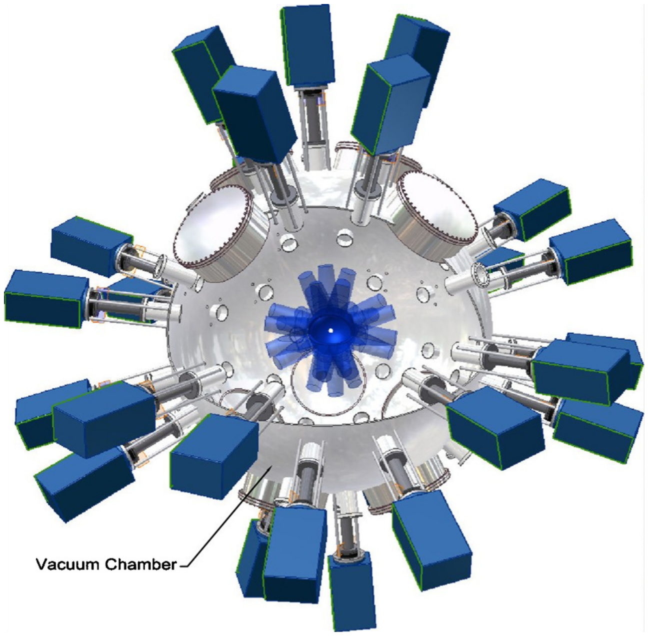

FIG. 2. (Color online) Illustration of the PLX, showing vacuum chamber, plasma guns and associated pulsed power capacitors mounted on small ports, and 60 cm diagnostic access ports. Converging jets and plasma liner are shown at center. Chamber diameter is 2.75 m.

by HyperV Technology Corp. are based on either minirailgun or coaxial accelerator concepts.[6] Jet parameters achieved so far are 8000 μg of Xe or Ar, launched at 50–70 km/s (Mach number, $M \sim 20-50$), $n \sim 10^{22}-10^{23}$ m^{-3}. Temperatures are $T_e \approx T_i \approx 1$ eV, and trapped magnetic flux $\sim 10^{-4}$ T.[6] High-Z gas (Xe and Ar) is utilized for (i) high momentum, and (ii) to keep T_i initially low (energy goes into ionization rather than heating), so that pressure is low until after the jets have merged to form the liner, and early time radiative losses are minimized.

II. DIAGNOSTIC ISSUES

The plasma will have three distinct regions. At the outer radii, individual jets will propagate from the chamber wall ($R \approx 137$ cm) to the merging radius, R_m, where they will encounter one another and begin to form a continuous liner shell. In PLX, R_m is predicted to be in the range of $R = 30-36$ cm, depending on jet parameters. Inside R_m, the merged jet liner will converge, pressure will increase, and inward velocity will reduce, until stagnation (zero radial velocity) is reached at the stagnation radius, R_s, which may occur around $R_s \sim 1$ cm. Table I shows the expected plasma parameters[7] in the three regions. As can be seen, there will be a predicted density increase of four to five orders of magnitude from the initial jet density to stagnation, and a temperature increase of $\sim 2-\frac{1}{2}$ orders of magnitude. Such extreme variations in expected parameters create a number of diagnostic challenges. Table II lists important physics issues (i.e., needed measurements) together with diagnostics planned to provide the measurements. Space precludes a detailed discussion of each of these key issues. However, some key points with respect to diagnostics can be addressed. First, each plasma gun will have its own set of basic diagnostics to ensure proper functioning on every shot, including a visible photodiode, dB/dt probe, current (Rogowski coil) and voltage monitors. The propagating jets will be covered by visible spectroscopy, fast imaging, and radially movable three-axis dB/dt probes operated on some shots to monitor jet-trapped magnetic flux. The low ion temperature in the individual jets will preclude spectroscopic Doppler broadening T_i measurements. However, supersonic jet velocities should be easily measurable with visible spectroscopy via Doppler shifts, even in the presence of large expected collisional line broadening.[8] Collisional (Stark) line broadening will also yield electron density. T_e measurements are expected to be possible in this region via line ratios, and the collisionality should be high enough that $T_i = T_e$. Tangent radial visible spectroscopic lines of sight that remain outside R_m are envisioned to diagnose this region. Additionally, a 1D visible photodiode array with imaging optics is planned to provide fast continuous imaging of jet propagation in the outer regions. Perhaps the most critical region in PLX will be around the merging radius, R_m, where the dynamics of the merging jets will determine to a great extent the viability of forming a uniform converging liner. Indeed, the first phase of PLX will be to investigate the merging dynamics of 2–5 jets, before moving to full 30 jet implosion experiments. For this reason, the main diagnostics effort, at least in the first phase of PLX, is directed at this region. Smoothed particle hydrodynamic modeling[7] indicates that lateral shock structures will form as individual jets encounter each other. This modeling also indicates that instabilities, such as Rayleigh–Taylor and Kelvin–Helmholtz modes, are not expected to occur on time scales of interest, because their growth rates are much slower than the hypersonic propagation speeds, and the formation time of lateral shock structures. Obviously, it is important for PLX to have sufficient measurements to test these theoretical predictions. Planned diagnostics to study the jet merging dynamics include an eight channel 632 nm interferometer with parts of the beam lines built in optical fiber to allow for relatively easy reconfigurability of the individual positions of chords. For example, chords may be laid out in a radial array along a jet, a transverse array at the merging radius, a 2D array across a merging region, etc. It will also be possible to

TABLE I. Expected plasma parameters in the three plasma regions. R_m=jet merging radius and R_s =stagnation radius, where the liner velocity$\rightarrow 0$.

Region	Radii	Expected parameters
Individual jets prior to merging	$R_m < R$	$n \sim 10^{21}-10^{22}$ m^{-3}; T_i, $T_e \sim 1$ eV
Jet merging, liner formation, initial compression	$R_s < R < R_r$	Changing
Stagnated high pressure plasma	$R \leq R_s$	$n \sim 10^{25}-10^{26}$ m^{-3}; T_i, Te>500 eV

TABLE II. PLX physics measurements and diagnostics.

Physics measurement	Diagnostic
Jet Mach number and transverse expansion prior to merging	Multichord interferometry (632 nm), visible frame imaging, fast diode array imaging, and Schlieren imaging
Merging physics (shock structure, liner thickness, shock heating, and instabilities)	Schlieren imaging, visible frame imaging, multichord interferometry (632 nm), visible spectroscopy, and pressure probe
Liner implosion/compression dynamics (liner thickness versus R)	Multichord interferometry (632 nm), Schlieren imaging, visible frame imaging, VUV spectroscopy, and pressure probe
Parameters at stagnation and after liner collapse, especially pressure, stagnation radius, and (equation of state) on axis	XRD array, bolometry, VUV spectroscopy, visible frame imaging, and crush ball pressure sensor
Jet trapped B-field	dB/dt probes
Plasma gun operation	dB/dt probe, Rogowski coil, photodiode, and voltage monitor (each gun)

position these chords to view the propagating jet region, $R > R_m$. The wavelength, 632 nm, was chosen after careful ray tracing calculations to optimize beam refraction and absorption versus phase shift in the merging region. The beam path will be tangent radial, entering and exiting through two opposite large access ports (cf. Fig. 2). Several imaging measurements focused around $R = R_m$ are also planned, including fast visible cameras (1.2 ns/frame two frame and 24 frame cameras), and Schlieren imaging[9] using a 1 J, 512 nm source laser and large reflective collection optics. VUV (vacuum ultraviolet) spectroscopy (50–300 nm) is also planned for this region, where the high density and initial low temperature will cause unacceptably short optical depths for visible wavelengths. For example, at $T_e = 10$ eV, $n = 10^{25}$ m^{-3}, the 1/e attenuation length estimated from free-free bremsstrahlung[8] is ≤ 1 cm for wavelengths $\lambda \geq 311$ nm. A tangent radial line of sight is planned for the VUV system (tangent at $R = R_m$). Doppler ion velocity measurements are planned and Doppler T_i measurements should be possible as the converging liner heats to tens of eV. Plasma parameters near and inside the stagnation radius are expected approach those of ICF (cf. Table I). In this region, diagnostics will for the most be restricted to passive light measurements in the EUV/SXR (extreme UV/soft x-ray) range. Background bremsstrahlung radiation and refraction will preclude the functioning of active measurements such as interferometry or Schlieren. EUV/SXR spectroscopy will be the workhorse diagnostic in this region to provide n_e and T_e via Stark broadening and line ratios. An array of x-ray PIN diodes (XRDs) with appropriate energy filters, located at several positions around the chamber is also planned in order to estimate peak T_e via the peak blackbody temperature (for $T > 100$ eV). The total radiated power, P_{rad}, can also be inferred from broad spectrum point XRD measurements, and since $P_{rad} = f(n_e n_i, Z^2, T_e)$,[8] $n_e n_i Z^2$ can be inferred if T_e is known via the blackbody estimate. Finally, a spherical "crush ball" as a rough measure of the stagnation pressure and symmetry is planned. The sphere will be suspended in the center of the target chamber. If it is stressed beyond its elastic limit, it will not return to its original shape at the end of the shot. For a spherical target and symmetric compression, the peak radial stress equals the applied hydrostatic pressure. Since most plastics and metals have limits of a few tens to a few hundred megapascals, the radial stress should easily surpass the elastic limit. Below the yield strength, the amount of expected deformation is roughly the stress divided by Young's modulus. Aluminum, for example, has a yield strength near 4 kbar and Young's modulus of about 700 kbar. A 2 cm radius sphere of aluminum subjected to static pressure slightly less than its yield strength would be expected to deform on the order of 0.1 mm. Careful measurement should reveal changes to the shape of the ball, even at relatively low pressures. The PLX experiment is currently under construction, and the plasma gun and pulsed power design is being finalized. Diagnostics discussed here are in the design and early construction phases. Two jet merging experiments are anticipated to begin summer 2011 and full 30 jet liner formation experiments will take place in late 2013 and 2014.

ACKNOWLEDGMENTS

This work is being supported by the U.S. Department of Energy, Office of Fusion Energy Sciences, High Energy Density Laboratory Physics program. The authors would also like to acknowledge the invaluable support of the other members of the PLX Team.

[1] Y. C. F. Thio, J. Phys.: Conf. Ser. **112**, 042084 (2008).
[2] M. M. Basko, A. J. Kemp, and J. Meyer-ter-Vehn, Nucl. Fusion **40**, 59 (2000).
[3] J. H. Degnan, M. L. Alme, B. S. Austin, J. D. Beason, S. K. Coffey, D. G. Gale, J. D. Graham, J. J. Havranek, T. W. Hussey, G. F. Kiuttu, B. B. Kreh, F. M. Lehr, R. A. Lewis, D. E. Lileikis, D. Morgan, C. A. Outten, R. E. Peterkin, Jr., D. Platts, N. F. Roderick, E. L. Ruden, U. Shumlak, G. A. Smith, W. Sommars, and P. J. Turchi, Phys. Rev. Lett. **82**, 2681 (1999).
[4] R. D. D. Ryutov and Y. C. F. Thio, Fusion Sci. Technol. **49**, 39 (2006).
[5] Y. C. F. Thio, C. E. Knapp, R. C. Kirkpatrick, R. E. Siemon, and P. J. Turchi, J. Fusion Energy **20**, 1 (2001); S. C. Hsu, *ibid.* **27**, 246 (2008).
[6] F. D. Witherspoon, A. Case, S. J. Messer, R. Bomgardner, M. W. Phillips, S. Brockington, and R. Elton, Rev. Sci. Instrum. **80**, 083506 (2009).
[7] J. T. Cassiby, R. J. Cortez, S. C. Hsu, and F. D. Witherspoon, Phys. Plasmas **16**, 112707 (2009).
[8] I. H. Hutchinson, *Principles of Plasma Diagnostics* (Cambridge University Press, New York, 1987).
[9] G. S. Settles, *Schlieren and Shadowgraph Techniques* (Springer, New York, 2001).